metals

MDPI

Review

A Review of Factors Affecting SCC Initiation and Propagation in Pipeline Carbon Steels

Shamsuddeen Ashurah Abubakar *, Stefano Mori and Joy Sumner

Centre for Energy Engineering, Energy and Sustainability Theme, School of Water, Energy and Environment, Cranfield University, Bedfordshire MK43 0AL, UK

* Correspondence: s.abubakar@cranfield.ac.uk; Tel.: +44-7762-667-474

Abstract: Pipelines have been installed and operated around the globe to transport oil and gas for decades. They are considered to be an effective, economic and safe means of transportation. The major concern in their operation is corrosion. Among the different forms of corrosion, stress corrosion cracking (SCC), which is caused by stresses induced by internal fluid flow or other external forces during the pipeline's operation, in combined action with the presence of a corrosive medium, can lead to pipeline failure. In this paper, an extensive review of different factors affecting SCC of pipeline steels in various environmental conditions is carried out to understand their impact. Several factors such as temperature, presence of oxidizers (O_2, CO_2, H_2S, etc.), composition and concentration of medium, pH, applied stress, and microstructure of the metal/alloy have been established to affect the SCC of pipeline steels. SCC susceptibility of a steel at a particular temperature strongly depends on the type and composition of the corrosive medium and microstructure. It was observed that pipeline steels with water quenched and quenched and tempered heat treatments, such as those that consist of acicular ferrite or bainitic ferrite grains, are more susceptible to SCC irrespective of solution type and composition. Applied stress, stress concentration and fluctuating stress facilitates SCC initiation and propagation. In general, the mechanisms for crack initiation and propagation in near-neutral solutions are anodic dissolution and hydrogen embrittlement.

Keywords: stress corrosion cracking; pipeline steels; applied stress; microstructure; anodic dissolution; hydrogen embrittlement

Citation: Abubakar, S.A.; Mori, S.; Sumner, J. A Review of Factors Affecting SCC Initiation and Propagation in Pipeline Carbon Steels. *Metals* **2022**, *12*, 1397. https://doi.org/10.3390/met12081397

Academic Editor: Luis Cáceres

Received: 14 June 2022
Accepted: 25 July 2022
Published: 22 August 2022

1. Introduction

Pipelines are intended to transport various types of fluids (liquid or gas), mixtures of fluids, solids, fluid–solid mixtures, or capsules (freight-laden vessels or vehicles moved by fluids through a pipe) [1]. They are considered to be a safe, effective and economic means of oil and gas transportation across the globe and have a good safety record [2,3]. However, they can suffer from corrosion.

Corrosion is defined as the destruction or deterioration of a metal that results from a reaction with its environment [4–6]. Corrosion in both offshore and onshore pipelines is a natural occurring phenomenon and is regarded as one of the major causes of pipeline failures [2,4], with corrosion damage accounting for about 20–40% of recorded pipeline failures and incidents [7]. In 2013, the National Association of Corrosion Engineers (NACE) estimated that the global cost of corrosion was USD 2.5 trillion, which is equivalent to 3.4% of the global gross domestic product (GDP) [8].

When pipelines are under stress, for example, from internal fluid movement or other outside forces, and are in the presence of a corrosive environment, they can be susceptible to stress corrosion, commonly known as stress corrosion cracking (SCC). Stress corrosion cracking is caused by the combined action of simultaneous mechanical stress and a specific corrosive media that a metal or alloy is susceptible to [6,9,10]. For SCC to occur on a metal or alloy surface, the following three conditions must be met simultaneously: specific

conditions to promote crack-propagation must be present; the metallurgy of the material must be susceptible to SCC; and there must be an applied tensile or static stress that exceeds a threshold value [10–12]. This tensile stress can originate from centrifugal forces, external loads, temperature variations or internal stresses induced by heat treatment. Stress may also result from locked-in residual stress from fabrication or welding [6,9,11]. SCC cracks normally propagate trans-granularly and/or inter-granularly or may be branched depending on the type of metal/corrosive media combination [9–12]. In the trans-granular mode of cracking, the crack advances without a defined preference for the grain boundaries, while in the intergranular mode, the crack proceeds along the grain boundaries.

Generally, two types of SCC have been outlined for pipeline carbon steels in the literature: high pH SCC and near-neutral pH SCC [13–17] High pH SCC is characterised by an intergranular mode of cracking and has been investigated in concentrated carbonate/bicarbonate environments with pH values higher than 9 [13–17]. Conversely, near-neutral SCC (pH = 6–8) is characterised by a trans-granular cracking mode and is associated with dilute carbonate/bicarbonate medium [13–17]. Figure 1a, b respectively shows examples of trans-granular and inter-granular SCC morphology on pipeline carbon steels.

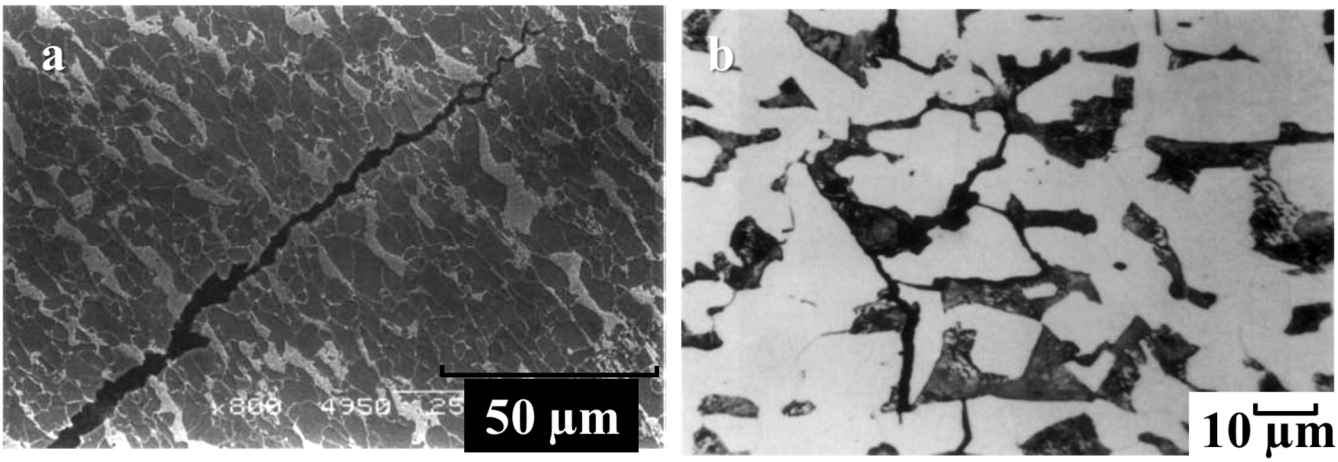

Figure 1. Typical SCC morphology on pipeline carbon steel surfaces; (**a**) trans-granular mode of SCC; (**b**) inter-granular mode of SCC [18]. Reprinted with permission from [18], 2011, John Wiley and Sons.

As shown in Figure 1a, the cracks on the steel surface propagate across the grain boundaries. This indicates a trans-granular mode of SCC with a continuous crack morphology. In Figure 1b, the cracks on the metal surface propagate along the grain boundaries. This indicates an intergranular mode of SCC with a discontinuous crack morphology.

The susceptibility of a metal to SCC is affected by several factors; namely: the chemical composition and microstructure of the alloy; the temperature of the environment; the presence of oxidizers in the corrosive medium (O_2, CO_2, H_2S, etc.); the composition and concentration of the corrosive medium; the stress; and the pH of the medium [6,12,19].

These factors are explored in more detail in the following sections with a brief introduction below. In terms of temperature dependence, SCC is accelerated by increasing temperatures as in most chemical reactions. However, the type of corrosive environment also determines the cracking behaviour of metals or alloys at a particular temperature [6,12]. The presence of oxidizers such as dissolved oxygen, carbon-dioxide or other oxidizing species (including ferric ions in corrosive environments) have a pronounced influence on the cracking susceptibility of metals or alloys [6,20,21]. These oxidizers, when present in high amounts, increase the aggressiveness of corrosive medium, by accelerating the oxidation reaction of the metals, leading to high anodic dissolution and subsequent failure [12,13,19]. Johnson et al. [22] stated that increasing CO_2 concentration from 0.5% to 25% in NS4 solution (near-neutral simulated soil) accelerates crack growth rate during cyclic loading.

Pipeline steels are made up of several types of microstructures; namely austenite, pearlite, ferrite, bainite, martensite, etc. Ferrite grains can further be classified into acicular ferrite, polygonal ferrite, allotriomorphic ferrite, globular ferrite and idiomorphic ferrite [23]. Microstructures that are more susceptible to SCC are characterised by high yield strength, high residual stress, high hardness, small and fine grain shapes and relatively low or entirely absent grain boundaries precipitates [6,24]. Low grain boundary precipitates result from low mill annealing temperature (T < 1000 °C). Mill annealing temperature also determines the grain size of a metal or alloy. Grain size decreases with decreasing mill annealing temperature [23].

The purpose of this paper is to conduct a critical review of these factors and their influence on SCC of pipeline steels in different operating environments, as this is the basis for understanding the corrosion behaviours of the pipeline steels prior to their installations and usage. It is essential to understand the effect of these factors on SCC of pipeline steels, as they play a vital role in setting up the most economical and effective corrosion mitigation strategies and hence will reduce corrosion related failures, leading to savings in production costs. The use of proper corrosion control practices can save up to 35% of the cost of corrosion in metallic structures [25]. Failure of these pipelines can impose serious risks to human life and can present economic and environmental problems.

2. Corrosion Mechanisms in a Near-Neutral pH SCC

The major corrosion mechanisms observed during SCC of pipeline carbon steels in a near-neutral solution are anodic dissolution and hydrogen embrittlement. Papavinasam [12], Sastri [11] and Cicek [9] defined hydrogen embrittlement as the loss or reduction of a metal's tensile strength and ductility due to diffusion of hydrogen atoms into the metal's crystalline structures during a corrosion process.

Figure 2 presents a typical example of hydrogen embrittlement on carbon steel. Hydrogen atoms are primarily produced from electrochemical processes such aqueous corrosion, acid pickling or electroplating. They can also be produced during the cathodic reduction reaction taking place during the corrosion process of metals in acidic solutions, such as hydrogen sulphide (H_2S) or hydrogen fluoride (HF) [10,12]. Hydrogen embrittlement causes premature brittle fracture of normally ductile metals under applied stresses less than the yield strength of the metal [10]. Hydrogen embrittlement of carbon steels commonly encountered in an aqueous medium involves CO_2. The corrosion reactions can be explained thus: CO_2 combines with H_2O to form H_2CO_3 (carbonic acid), H_2CO_3 then further dissociates into HCO_3^-, H^+ and CO_3^{2-} [26,27]. The major cathodic reactions are the reduction of H^+, H_2CO_3 and HCO_3^- as expressed below [28,29]:

$$2H^+_{(aq)} + 2e^- \rightarrow H_{2(g)} \quad (1)$$

$$2H_2CO_{3(aq)} + 2e^- \rightarrow 2HCO_3^-{}_{(aq)} + H_{2(g)} \quad (2)$$

$$2HCO_3^-{}_{(aq)} + 2e \rightarrow 2CO_3^{2-}{}_{(aq)} + H_{2(g)} \quad (3)$$

$$2H_2O_{(l)} + 2e^- \rightarrow 2OH^- + H_{2(g)} \quad (4)$$

According to Nesic et al. [28] and Mu and Zhao [29], the reduction of H_2CO_3 and HCO_3^- is the dominant reaction at pH values of 4–6 in aqueous CO_2 medium, whereas the H^+ reduction reaction is more significant at lower pH values. The major anodic reactions are the dissolution of Fe (iron) followed by $FeCO_3$ (iron carbonate) formation as shown below [28,29]:

$$Fe \rightarrow Fe^{2+} + 2e^- \quad (5)$$

$$Fe^{2+} + CO_3^{2-} \rightarrow FeCO_3 \quad (6)$$

Anodic dissolution, also known as metal dissolution, is a process in which the metal is dissolved from the anodic site during corrosion processes, and gases are released from the cathodic site and at the metal surface [30]. The rate of metal dissolution in an electrochemi-

cal reaction is higher when it is in an active state in comparison to the passive state. It also depends on the corrosive medium's composition and environmental conditions [6].

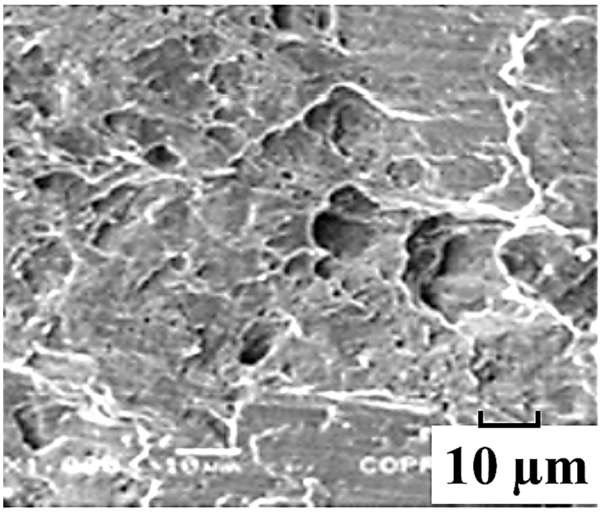

Figure 2. A typical example of hydrogen embrittlement on X46 carbon steel [15]. Reprinted with permission from [15], 2014, Elsevier.

3. Common Pipeline Steels and Operating Conditions

The most common pipeline steels currently installed and operated in various locations around the world, both onshore and offshore, include API 5L X65, X70 and X80. Currently, grade X70 and X80 carbon steels are being used in subsea pipelines for non-sour fluid service, and grade X65 is presently the most established pipeline material operating in sour fluid service. A X70 pipeline has been installed and operated by Statoil and British Petroleum in the North Sea. It is also installed by Shell Oil Mensa in the Gulf of Mexico [31,32]. The use of grade X80 for export pipelines in offshore applications has been assessed and qualified by a joint industry project called EXPIRE (Project conducted by Statoil, Europipe line pipe company and J P Kenny design office) [31,32].

The number after each API 5L grade carbon steel represents its yield strength in thousand psi, for example in X65 grade (65-represents 65,000 psi). The chemical compositions of API 5L X65, X70 and X80 are presented in Table 1. The SCC susceptibility of these pipeline steels, as presently tested under various environmental conditions and reported in the wider LITERATURE, are summarised in Table 2.

Table 1. Chemical compositions of API 5L X65, X70 and X80 pipeline steel (wt.%). [14,33]. Reprinted with permission from [14,33], 2008, 2019, Elsevier.

Material Grade	C	Mn	Si	S	P	Mo	Cr	Cu	Ti	V	Ni	Fe
X65	0.10	1.43	0.19	0.001	0.007	0.16	0.12	0.07	-	0.09	-	97.832
X70	0.027	1.51	0.10	0.002	0.014	0.004	0.27	0.28	0.011	-	0.16	97.494
X80	0.06	1.91	0.35	0.001	0.013	0.157	0.201	0.023	0.017	0.001	0.036	97.231

Table 2. SCC susceptibility test environmental conditions. Data from [14,16,33].

Material Grades	Test Environmental Conditions	
	Temperatures, °C	Test Solutions Composition
X46, X52, X65, X70, X80, X90, X100.	5, 15, 25, 30, 35, 50, 55, 60, 70, 90.	Air, NaCl solutions (3.5% NaCl), NS4 solution, Bicarbonate solutions ($NaHCO_3$), NACE solution (5% NaCl + 0.5% acetic acid), CO_2, O_2, CO_2 + O_2, CO_2 + N_2, CO_2 + H_2O, O_2 + H_2O, Simulated fuel grade ethanol (SFGE), etc.

4. Common SCC Assessment Techniques

Laboratory assessment used to detect and evaluate SCC (in addition to general, localized, pitting corrosion, etc.) consists of two main stages [12], namely; the laboratory test methodology and corrosion monitoring technique. The laboratory test methodology includes the equipment used to simulate the corrosion variables, while the monitoring technique is used to determine the corrosion effect or rate that is been induced. Table 3 presents commonly used SCC monitoring techniques. The most common stress or load application systems used to determine the stress resistance of a metal in the laboratory are presented in Table 4. Not all corrosion monitoring techniques are suitable for all laboratory test methodologies [12].

Table 3. Common electrochemical monitoring techniques. Data from [12,33,34].

Electrochemical Monitoring Techniques	
Linear polarization resistance (LPR)	Measures the electrochemical response (resistance) of a working electrode (corroding metal) near its open circuit potential. It involves the polarization of ±10 mV around corrosion potential.
Electrochemical impedance spectroscopy (EIS)	Involves application of AC potential of ±10 mV around corrosion potential, over a wide frequency range, typically 0.1 to 10^6 Hz. It is used to obtain corrosion current.
Electrochemical noise (EN)	This method continuously measures corrosion potential and current fluctuations. It is used to obtain corrosion current from noise resistance.
Cyclic potentiodynamic polarization	Involves the application of overpotential from around corrosion potential towards the noble side to a potential at which 5 mA current is reached, and then the potential is reversed until corrosion potential is achieved.

Table 4. Common stress application methods. Data from [12,35,36].

Stress Application Methods	
Dynamic load test (slow strain rate test), e.g., round tensile and tube.	Considered the most widely used test for assessing the susceptibility of a metal to SCC. It is conducted by continuously increasing the applied stress level at a constant strain rate.
Constant load test, e.g., notched beam, direct tension specimens.	This method is usually used when the load to be applied on the specimen is small; normally, a hanging weight is suspended on the specimen.
Cyclic load test, e.g., bent beam, notched beam samples.	In this method, a repeated or fluctuating stress is applied on the specimens at a particular point.
Deflected method (Constant strain), e.g., C-ring, bent-beam, U-bend samples.	In this method, stress is applied on the specimen by deflecting it. In deflected test samples, the applied stress decreases as crack propagates.

5. Effect of Microstructure on SCC of Pipeline Steels

The susceptibility of a metal or alloy to SCC is affected by its chemical composition and microstructure [6,10,11]. Several types of microstructures are observed in pipeline steels including, austenite, pearlite, ferrite, bainite and martensite. Depending on the cooling rate and nucleate content, different forms of ferrite grains can nucleate such as acicular ferrite, polygonal ferrite, allotriomorphic ferrite, globular ferrite and idiomorphic ferrite [23]. Acicular ferrite, which is a thin needle-like form of ferrite grain, has been understood to be the optimum microstructure with a combination of good toughness and high strength, which is mainly due to its fine-grained nature and high density of dislocations [37,38] Metals with under-tempered martensitic or bainitic microstructures or those without post-weld heat treatment in the heat affected zones are found to be less resistant to SCC [39] SCC susceptibility of a metal can be predicted based on yield strength

and grain size, since better resistance was observed in metals with lower yield strength and larger grain sizes [40]. According to Sastri [11], the amount of carbon and its distribution in a steel matrix are important factors controlling the resistance of a metal or alloy to SCC. The threshold stress for crack initiation was found to depend on the amount of carbon in the steel. Regular steels tend to be less resistant to SCC when the carbon percentage is below 0.1 wt.%, while ferritic steels with chromium contents of about 18% to 20% have higher resistance to SCC [11]. The effect of microstructure on SCC of pipeline steels in various environmental conditions have been reported by several researchers as discussed in the subsequent paragraphs.

Torres-Islas et al. [14] evaluated the SCC behaviour of a X70 micro-alloyed pipeline steel, with different microstructures as presented in Table 5.

Table 5. Different microstructures of the X70 micro-alloyed pipeline carbon steel. Data from [14].

Heat Treatment	Microstructure
As-received sample	Ferrite grains with pearlite alternation
Quenched and tempered	Incipient acicular ferrite with isolated perlite grains
Water-sprayed (cooled)	Incomplete transformation of perlite in a recrystallized ferrite matrix
Water quenched	Typical microstructure of martensite with segregation at martensitic lath boundaries

The tests were conducted at 50 °C in different concentrations of $NaHCO_3$ solution (0.1, 0.05, 0.01 and 0.005 M) by use of slow strain rate test (SSRT) with a strain rate of 1.36×10^{-6} in/s and in air. In these tests, different potentials of 100 mV saturated calomel electrode (SCE), 200 mV (SCE), and 300 mV (SCE) more anodic and 100 mV (SCE), 200 mV (SCE), 600 mV (SCE), and 1600 mV (SCE) more cathodic than their rest potential (E_{corr}) were applied. The tests results indicated that the specimen exposed in the most diluted solution of $NaHCO_3$ has the highest loss of ductility and was most susceptible to SCC irrespective of the alloy's microstructure. In the diluted $NaHCO_3$ solution, applied cathodic potentials close to their free corrosion potential decreased the SCC susceptibility of the specimens regardless of the microstructure, whereas higher applied cathodic potentials increase SCC susceptibility in all sample microstructures. In addition, the higher the cathodic potential applied, the lower the percentage reduction in cross-section area, leading to higher susceptibility of the test specimen to SCC. According to the percentage reduction in area, hydrogen ingress into the alloy's crystal lattice affected quenched and quenched-tempered specimens both in air and in the most diluted concentration of $NaHCO_3$. This shows that hydrogen ingress had a higher effect on the reduction in ductility on the quenched and quenched-tempered specimens. Trans-granular cracks were observed in the quenched-tempered specimen. Gonzalez-Rodriguez et al. [41] observed similar results when they tested SCC susceptibility of X80 carbon steel with different heat treatments (water quenched, quenched and tempered, water sprayed, and as received state) in different $NaHCO_3$ solutions (0.01 M and 0.05 M) at room temperature. Table 6 presents the different microstructures observed after the heat treatments.

Table 6. Different microstructures of the X80 pipeline carbon steel. Data from [41].

Heat Treatment	Microstructure
As-received sample	Ferrite and pearlite bands with dispersion of precipitates.
Quenched and tempered	Partially recrystallized grains with incipient acicular ferrite and isolated pearlite grains.
Water-sprayed	Incomplete transformation of perlite grains with few precipitates.
Water quenched	Martensite with high segregation at martensitic lath boundaries and dispersion of precipitates.

The tests results indicated that the X80 carbon steel samples are more susceptible to SCC in 0.01 M $NaHCO_3$ solution (the lowest concentration) irrespective of alloy's

microstructure. The quenched specimens were observed to show highest SCC susceptibility followed by the quenched and tempered specimens, whereas the as-received samples showed the least SCC susceptibility.

Liu et al. [42] evaluated the SCC behaviour of API 5L X70 pipeline steel with different applied heat treatments and microstructures as presented in Table 7. The tests were conducted by use of the SSRT method with a strain rate of 5×10^{-7} in/s in an acidic soil extract (pH of 4.41) collected from 1.5 m underground. Cathodic potentials of −650 mV (SCE), −850 mV (SCE) and −1200 mV (SCE) below the corrosion potential were applied in these tests. The tests results indicated a mixed-mode of SCC mechanism, caused by anodic dissolution and hydrogen embrittlement. The water quenched specimen with bainite grains had a higher susceptibility to SCC in the acidic soil extracts, while the as-received sample with ferrite matrix grains had a lower susceptibility to SCC. It was observed that the SCC mechanism changed with varying applied potentials. At a lower negative applied potential, the specimen's cracking mechanism was based mainly on anodic dissolution. When the applied potential was more negative, hydrogen was involved in the cracking process, and trans-granular cracks were observed. With the application of more negative potentials, the SCC mechanism was completely based on hydrogen-induced mechanism, with a river-bed shaped brittle feature of the fractured surface.

Table 7. Different microstructures of the exposed X70 samples. Data from [42].

Heat Treatment	Microstructure
As-received	Ferrite matrix grain with dark martensite/austenite grains
Air-cooled	Coarse ferrite grains with a number of granular bainite grains
Water quenched	Bainite grains

Fu et al. [43] observed similar results when they tested X70 carbon steel at different applied cathodic potentials below E_{corr} in a simulated soil solution using the SSRT technique. The test results showed that, at an applied potential of −450 mV (SCE), the mechanism of SCC was anodic dissolution; however, when the potential was decreased to −850 mV (SCE), the anodic dissolution of the X70 steel was inhibited, and when a potential of −1200 mV (SCE) was applied, the specimens showed a higher SCC susceptibility, and the mechanism of SCC was purely by hydrogen embrittlement.

Similar results were reported by Jeffrey et al. [24] for X70 water quenched specimens tested in an NS4 solution with a pH of 6.7. The quenched specimens with acicular and polygonal ferrite grain microstructure were observed to be more susceptible to SCC. Bulger et al. [44] also observed similar results of higher SCC susceptibility of quenched X70 carbon steel with bainitic microstructure in comparison with annealed and normalised samples with both ferritic/pearlitic microstructures tested in NS4 solution. Zhu et al. [45] investigated the SCC behaviour of high strength X80 pipeline steel with fine acicular ferrite and granular bainite microstructure in comparison with a low strength X65 carbon steel, which consisted of ferrite/pearlite microstructure in high pH carbonate/bicarbonate solution. The X80 steel was found to exhibit higher SCC susceptibility than the X65 steel.

Jeffrey et al. [24] used the SSRT technique to study the SCC susceptibility of different microstructures of X70 carbon steel as shown in Table 8. According to the calculated area reduction ratio (RRA = (area ratio in NS4/area ratio in air)), the annealed specimens had the highest resistance to SCC, whereas the water quenched specimens showed the greatest SCC susceptibility. Figure 3 shows the variation in SCC susceptibility of the different microstructural samples in relation to area reduction ratio. The annealed microstructure was observed to have a larger grain size as compared with the normalised samples and as such showed an increased resistance to SCC. The effect of grain size extended to the water quenched specimens which had smaller grain sizes and showed lower resistances to SCC.

Table 8. Different microstructures of the exposed X70 samples. Data from [24].

Heat Treatment	Microstructure
Mill annealed	Ferritic/pearlitic grains
Normalized	Ferritic/pearlitic grains
Water quenched	Acicular and polygonal ferrite grains
Quenched and tempered	Displayed coarsening of the quenched microstructure with some degree of recrystallization

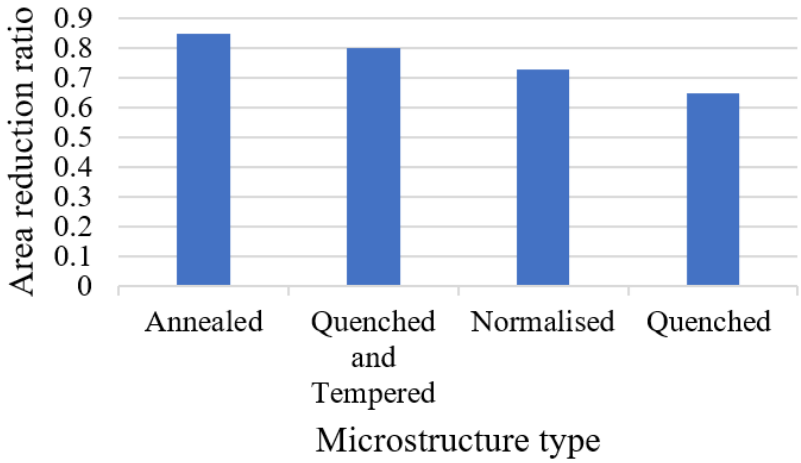

Figure 3. Variations in SCC susceptibility of the different microstructural tested samples. Data from [24].

Lu and Luo [46] evaluated the relationship between yield strength and microstructure on SCC resistance of different grades of pipeline steels with different microstructures in a near-neutral solution. The test material grades consist of API 5L X52, X60, X65, X70, X80 and X100. The X52, X60, and X65 steels were made up of ferrite + pearlite microstructures, while the X70, X80, and X100 steels consisted of fine-grained bainite + ferrite microstructures. The SSRT technique was used to assess the SCC susceptibility of the samples at a strain rate of 10^{-7} in/s in an NS4 solution saturated with 95% N_2 + 5% CO_2 to create a near-neutral pH value (pH 6.7). The tests results indicated that near-neutral pH SCC susceptibility of pipeline carbon steels generally increases with an increase in yield strength level, but the strength dependence of SCC resistance is highly affected by the microstructures of the steels. SEM images on the fractured surfaces of the specimens revealed a trans-granular SCC appearance in some areas and many cavities produced by the micro-plastic deformation were observed.

Recent research has shown that the application of cyclic quenching and/or tempering heat treatments have high potential for enhancing the mechanical properties of carbon steels due to formation of finer grain microstructure. Hafeez et al. [47] investigated the corrosion behaviour and mechanical properties of a low-alloy carbon steel under different cyclic heat treatments such as single quenching and tempering (SQT), cyclic double quenching and tempering (CDQT) and cyclic triple quenching and tempering (CTQT). Tests results by X-ray diffraction analysis revealed the formation of ε–carbide (Fe2.4C) on the CDQT and CTQT heat treated specimens which provided nucleation sites for formation of a reformed austenitic grains. This resulted in the formation of a more saturated lath martensite and a refined austenite grain. Mechanical tests results of the CDQT and CTQT specimens showed a 19% increase in tensile strength with a 100% elongation in comparison to the SQT. Higher ductility was observed in the CDQT and CTQT specimens than SQT.

Kang et al. [48] assessed the effect of tempering on the mechanical properties of a medium carbon bainitic steel by isothermal transformation and tempering between 240–450 °C. A plate-like bainitic ferrite grain with thin-like refined austenite were obtained after the heat treatments. The tests results revealed that specimens tempered at 340 °C

presented the most optimum toughness and strength level with an increase in plasticity. The specimens tempered at 320 and 360 °C, respectively, showed lower and high yield values. However, when the temperature was increased to 450 °C, a coarsened bainitic ferrite grain with carbide precipitation was observed on the samples. This results in low toughness of the specimen. It was observed that the quantity of the retained austenite increases with increasing temperature to below 400 °C, with a decrease as the tempering temperature is increased to above 400 °C. In conclusion, it can be stated that with increasing tempering temperature, the austenite grain further transforms into bainitic grain and decomposes into carbide, thus reducing the toughness and strength of the samples.

In summary, it was observed that pipeline carbon steels with water quenched, and quenched and tempered heat treatments, and that consist of acicular ferrite, bainitic ferrite or martensitic microstructures are more susceptible to SCC irrespective of solution type and composition. Tempering heat treatments have the potential to improve the mechanical properties of carbon steels.

6. Effect of Corrosive Medium Composition and Concentration on SCC of Pipeline Steels

Most alloys are susceptible to stress corrosion in specific corrosive environments [6]. In general, not all alloy-corrosive medium composition combinations will induce SCC [6]. For example, carbon steel is susceptible to SCC in strong alkaline solutions and when nitrates are present in the solutions but not in strong acid solutions. Stainless steels are susceptible to SCC in caustics and chloride-containing solutions but not in nitric acid, sulfuric acid or pure H_2O [6,9,12]. SCC is well known to occur in various aqueous solutions, and it is also influenced by the presence of oxidizers such as oxygen, carbon-dioxide, hydrogen sulphide, etc. [6,12]. For example, the presence of dissolved oxygen or other oxidizers in a chloride environment is critical to the cracking tendency of austenitic stainless steels and, if the oxidizer or oxygen is eliminated, cracking will not take place [6]. Several laboratory studies have been carried out to assess the susceptibility of different pipeline steels to SCC by simulating various environmental conditions as discussed below.

Omura et al. [17] assessed the susceptibility of X65 and X80 pipeline steels at 25 °C in different test solution compositions of 1 g/L $NaHCO_3$ with either no gas, the solution saturated with CO_2, or in solution saturated with air and CO_2. These tests were conducted at the open circuit potential and at a strain rate of 1×10^{-6} in/s. The tests results were evaluated based on fracture elongation (EI) and area reduction (RA) of the specimens. Significant reductions in EI and RA were observed in all the test solutions as compared to the test in air. Relative differences in EI and RA were observed in the solution saturated with CO_2 and mixture of air and CO_2. Secondary cracks and a loss in ductility were observed on all the samples, and EI and RA values were also different between the alloys. The tests results showed that SCC can occur with or without application of cathodic potential when under the influence of severe stress–strain conditions.

Bueno et al. [15] used the SSRT technique to evaluate the cracking resistance of API 5L X46 carbon steel in air, NS4 solution and aqueous extracts from soil samples at 25 °C. Tables 9 and 10, respectively, present the standard composition of NS4 solution and the chemical composition of the X46 carbon steel. In these tests, different cathodic potentials of 100 mV (SCE) and 300 mV (SCE) below corrosion potential (E_{corr}) were applied with strain rates of 9×10^{-6} in/s and 9×10^{-7}in/s. Figure 4 shows the variations in time to failure of the specimens in the different solutions with the influence of applied cathodic potentials. Lower time to failure was observed at applied potential of 300 mV (SCE) below the corrosion potential in both soil extracts and NS4 solution. The tests results indicated trans-granular cracks in the specimens with decreasing ductility as higher cathodic potentials are applied. It was observed that cracking occurred by SCC, but hydrogen generated from the applied cathodic potential contributed to the initiation and crack propagation of the specimens. Furthermore, it is also observed that specimens tested with a strain rate of 9×10^{-7}in/s had higher loss of ductility than those tested with strain rate of 9×10^{-6} in/s.

This behaviour can be attributed to hydrogen diffusion in the specimens because of the longer exposure times they are subjected to before failure. Rebak et al. [49] reported similar results of SCC susceptibility on X52 pipeline steel tested in NS4 solution by use of constant extension rate tests at different applied cathodic potentials. The tests results indicated that SCC susceptibility was at minimal near E_{corr} and increased with increasing cathodic potential. Similar results were also observed by Contreras et al. [50] on X52 carbon steel tested in NS4 solution by use of the SSR technique at different applied cathodic potentials. The electrochemical impedance spectroscopy (EIS) tests results showed that the highest corrosion of the specimens was obtained at the highest applied cathodic potential of −400 mV (SCE). As shown in Figure 5, a brittle type of fracture with trans-granular appearance was observed on the exposed specimen, which commonly occurred due to hydrogen embrittlement.

Table 9. Standard chemical composition of NS4 (near-neutral synthetic soil) solution [50]. Reprinted with permission from [50], 2012, Elsevier.

Substance	KCl	$NaHCO_3$	$CaCl_2 \cdot 2H_2O$	$MgSO_4 \cdot 7H_2O$
Concentrations (g/L)	0.122	0.483	0.181	0.131

Table 10. Chemical composition of X46 carbon steel (wt.%) [15]. Reprinted with permission from [15], 2014, Elsevier.

Material Grade	C	Mn	Si	Cr	Ni	Mo	S	P	Fe
API 5L X46	0.25	1.28	0.34	0.02	0.01	0.03	0.009	0.014	Bal.

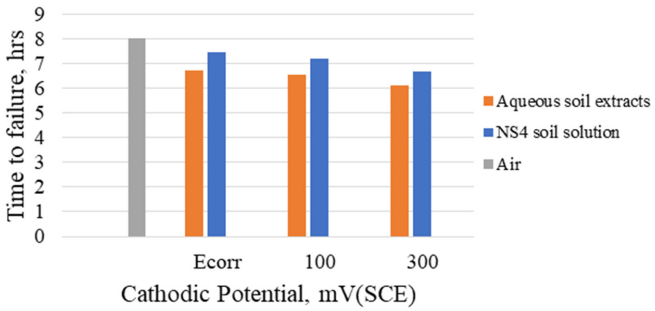

Figure 4. Variations in time to failure of the API 5L X46 exposed samples in air, aqueous soil extracts and NS4 solution at open circuit potential (Ecorr), 100 mV (SCE) and 300 mV (SCE) below corrosion potential. Data from [15].

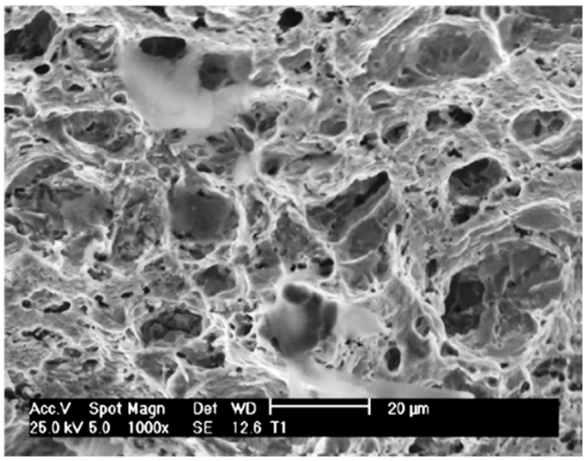

Figure 5. SEM images showing a trans-granular fracture on exposed specimens in the NS4 solution with applied potential of −400 mV (SCE) [50]. Reprinted with permission from [50], 2012, Elsevier.

Nevertheless, Zhang et al. [51] investigated the degree of hydrogen embrittlement of API 5L X70 in comparison with X80 and X90 high-strength carbon steels under cathodic protection in simulated soil solutions. The results from the hydrogen permeation tests showed an increasing hydrogen diffusion rate and concentration on the steel surfaces with increasing tensile strength of materials under the different cathodic protections levels. Figure 6 shows the correlative calculated hydrogen permeation parameters of the different steel grades. A decreasing percentage of area reduction was also observed with an increase in material's tensile strength in the different test conditions.

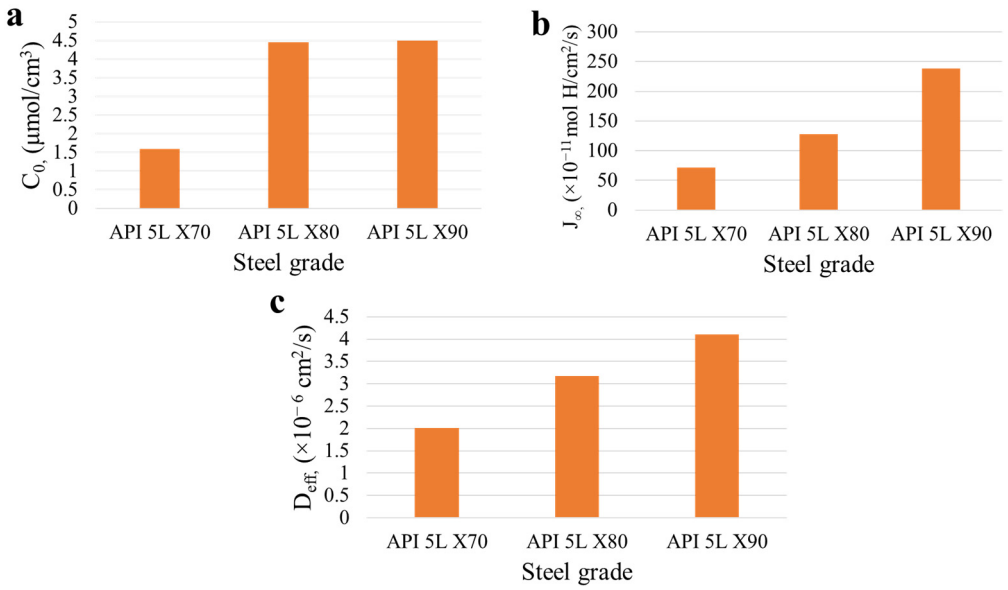

Figure 6. Calculated hydrogen permeation parameters of the different steel grades under applied cathodic potential of −1200 mV (SCE); (**a**) hydrogen concentration (C_0); (**b**) hydrogen permeation flux (J_∞); (**c**) effective hydrogen diffusion (D_{eff}). Data from [51].

As shown in Figure 6a–c, the surface hydrogen concentration (C_0), hydrogen permeation flux (J_∞) and effective hydrogen diffusion (D_{eff}) increased with increasing materials' tensile strength. This clearly shows that the rate of hydrogen accumulation and uptake is higher in higher strength steels and can lead to greater susceptibility to hydrogen embrittlement and hence higher SCC susceptibility.

Majchrowicz et al. [16] investigated the cracking susceptibility of P110 pipeline steel in CO_2-rich medium (pure CO_2 and CO_2/H_2O). Table 11 presents the chemical composition of the P110 pipeline steel. The SCC susceptibility was tested by use of U-bended samples, tensile tests of miniaturized samples cut from the exposed U-bend specimens and SSRT tests at different strain rates of 10^{-4} in/s, 10^{-5} in/s and 2×10^{-6} in/s. Results from the SEM assessment showed no clear long visible SCC cracks on any of the specimens exposed to CO_2 and wet CO_2 (CO_2/H_2O). However, corrosion pits with micro-cracks were observed in the vicinity of the deformed sections of the U-bended specimens. Small cracks with brittle fracture were also observed in the SSRT specimens in the wet CO_2 environment tested at a strain rate of 2×10^{-6} in/s. This confirms the possibility of SCC occurrence. Tensile tests of miniaturized samples cut from the deformed section of U-bend specimens indicated a significant reduction in ductility in both the CO_2 and CO_2/H_2O medium. In conclusion, the SSRT and tensile tests of the miniaturized samples cut from U-bend specimens clearly indicated that P110 steel is susceptible to SCC in CO_2-rich medium and that this is associated with anodic dissolution and hydrogen embrittlement.

Table 11. Chemical composition of the P110 pipeline steel (wt.%) [16]. Reprinted with permission from [16], 2019, Elsevier.

Material Grade	C	Mn	Si	S	P	Fe
P110	0.243	0.990	0.196	0.002	0.014	Bal.

Zhang et al. [52] used the SSRT technique at a strain rate of 1×10^{-6} in/s to evaluate the SCC susceptibility of API 5L X70 carbon steel in various CO_2 concentrations. Increasing CO_2 concentrations of 0%, 5%, 10%, 15%, 20% and 100% balanced with nitrogen gas in soil extracts solution were used for the tests. The tests results indicated a rapid fall in area reduction of specimens with increasing CO_2 concentration. The susceptibility of the specimens to SCC increased with increasing CO_2 partial pressure until a steady state value was reached at about 20% CO_2 concentration. A similar outcome was reported by Johnson et al. [22] for API 5L X65 pipeline steel which showed that increasing CO_2 concentration from 0.5% to 25% in NS4 solution facilitates its fatigue crack propagation rate during cyclic loading. Furthermore, the brittleness of the fractured specimens increases with the CO_2 partial pressure. This is attributed to ingress of hydrogen atoms into the steel's crystalline structure, thus decreasing its ductility and hence facilitating crack propagation. Figure 7a–c shows the effect of increasing amounts of CO_2 on the electrochemical parameters measured during the electrochemical tests. It is clear that with increasing CO_2 concentration polarization, resistance (R_p) decreases, pH of the solution decreases and corrosion current density (I_{corr}) increases. Jeffrey et al. [53] and Asher and Singh [54] also observed a decrease in solution pH with increasing CO_2 concentration in a simulated carbonate/bicarbonate solution used to assess SCC behaviour of X65 carbon steel. However, it was observed that application of cathodic protection increases the pH at the steel surfaces, shifting the medium away from near-neutral pH conditions [54].

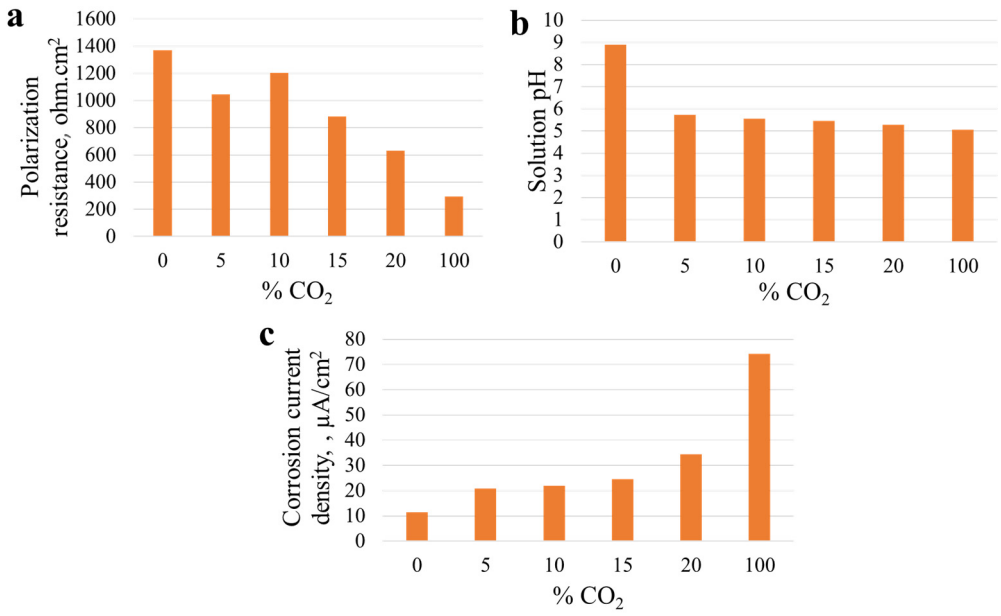

Figure 7. Effect of increasing CO_2 content on the measured electrochemical parameters; (**a**) polarization resistance; (**b**) solution pH; (**c**) corrosion current density. Data from [52].

Nevertheless, Johnson et al. [22] evaluated the cracking susceptibility of API 5L X65 pipeline steel by use of cyclic loading tests in a simulated NS4 solution with varying concentrations of CO_2 and O_2 at 35 °C. The tests results showed that with increasing amount of CO_2, corrosion rate and hydrogen permeation increased, as well as accelerated crack propagation during the cyclic loading tests. A measure of the crack length over time indicated well-defined increase in crack velocity with increasing CO_2 content between

0 and 5%. The effects of O_2 concentration on corrosion rate were small in comparison with CO_2, increasing the amount of O_2 decreased the hydrogen permeation rate and increased crack propagation rates during crack growth test. Crack velocity decreased slightly with the addition of 1% O_2 to the N_2 gas, while 10% and 20% O_2 increased the crack propagation rate. The effect of O_2 concentration on hydrogen permeation rate was anticipated in that O_2 increased the rest corrosion potential, while reducing the rate of reduction reactions that generate hydrogen atoms. Gu et al. [55] also observed in an SCC susceptibility test on X-52 and X-80 carbon steels in a near-neutral aqueous solution that increasing CO_2 concentration accelerates SCC occurrence on the specimens. This suggests that anodic dissolution and hydrogen embrittlement are involved in the SCC process [55].

In summary, it was observed that SCC of pipeline steels in a near-neutral solution varies with solution composition, concentration of oxidizers and their applied partial pressure. It is clear that with increasing CO_2 concentration, polarization resistance (R_p) decreases, which in turn increases corrosion rate, hence facilitating SCC occurrence. The severity of SCC occurrence increases with increasing applied cathodic potential. In general, the mechanism for crack initiation and propagation in various concentrations of O_2 and CO_2 constitute anodic dissolution and hydrogen embrittlement.

7. Effect of Temperature on SCC of Pipeline Steels

Temperature increases the rate of most chemical processes or reactions. In general, an increase in temperature will result in an increase in corrosion rate [9]. According to Sastri [11], the corrosion rate of steel in acid solutions doubles for an increase of 10 °C between 15 and 70 °C. Increases in temperature increase the diffusion of oxygen through the oxide film on metal or alloy surfaces [56]. However, the solubility of oxygen or carbon dioxide in aqueous solutions is lower at temperatures above 70 °C or in some cases 80 °C, and therefore, the rate of reaction cannot be doubled [9,11]. Temperature determines the cracking behaviour of metals or alloys, which also depends on the type and composition of the corrosive medium [6]. In some environments, cracking occurs readily at room temperature, while in some other systems, boiling temperatures are required [6]. Most alloys that are susceptible to SCC will begin cracking at least as low as 100 °C [6,12]. The effect of temperature on SCC of pipeline steels in various environmental conditions has been assessed by several researchers as discussed in the subsequent paragraphs.

Contreras et al. [57] evaluated the SCC susceptibility and cracking mechanism of API 5L X60 pipeline steel to SCC by use of the SSRT method at a strain rate of 1×10^{-6} in/s. The tests were conducted in a glass autoclave filled with NS4 solution at varying pH level of 3 and 10 at room temperature (24 °C) and 50 °C. According to the calculated area reduction and time to failure ratios, the samples were less resistant to SCC at pH 3 irrespective of the solution temperature. The SCC susceptibility was observed to be higher at 50 °C at pH 10. The SCC failed specimens were observed to have a brittle type of fracture with transgranular cracking mechanism. The SCC mechanism of the samples in the NS4 solution was a combination of anodic dissolution and hydrogen-based mechanism.

Asher et al. [58] investigated the SCC susceptibility of X-65 pipeline steel by use of the SSR technique in varying bicarbonate concentrations of 0.1 g/L, 0.5 g/L and 1 g/L bubbled with 5% CO_2 at different temperatures of 15, 25 and 35 °C. The SCC susceptibility of the samples was measured based on the calculated crack velocity. Highest crack velocity was observed in the solution with 0.5 g/L $NaHCO_3$ at 15 °C and lowest at 25 °C with 0.5 g/L $NaHCO_3$.

Ye et al. [59] studied the susceptibility of X70 carbon steel to SCC by use of slow strain rate technique. The tests were carried out in NACE solution (5% NaCl + 0.5% acetic acid) at room temperature (25 °C) and 60 °C. The tests results indicated lower SCC sensitivity at room temperature. When the temperature was increased to 60 °C, the stress corrosion cracking sensitivity increased, and showed clear tendency to stress corrosion. Faster movement of Cl^- and O_2 was observed in the solution at 60 °C; this leads to change in SCC sensitivity, as oxygen diffusion plays a vital role in accelerating SCC occurrence. Fragiel

et al. [60] evaluated the SCC resistance of two API 5L X65 micro-alloyed pipeline steels with ferritic–pearlitic and martensitic microstructures by use of constant displacement in NACE solution at room temperature and 55 °C. The tests results indicated that at room temperature, the X65 samples with a ferritic–pearlitic microstructure showed crack tip dissolution, with trans-granular crack mode and some evidence of hydrogen embrittlement, decohesion between grain boundaries was also observed, as well as some cavitation at the front of the crack tip. The material with martensitic microstructure exposed at room temperature showed a mixed trans-granular-intergranular cracking mode; no cavitation at the crack tip was observed. At 55 °C, trans-granular cracks were observed for both tested specimens, with cracks longer than those observed at room temperature. This indicates some involvement of hydrogen mechanisms, most likely thermally activated, in addition to the anodic dissolution. According to the measured threshold stress intensity factors (K_{iscc}) in the exposed conditions, both specimens were resistant to SCC. Ramirez et al. [61] studied the SSC susceptibility of newly developed micro-alloyed pipeline steel (C-Mn steel) with different microstructures of ferritic, martensitic, and ferritic/bainitic alloys. SSRT technique was used to assess their SSC susceptibility at a strain rate of 1×10^{-6} in/s at 25, 50, 70 and 90 °C (±3 °C) in a NACE solution. The tests results indicated that in all the exposed conditions, the percentage reduction in area and number of hydrogen atoms at the surface increased with increasing temperature. Figures 8 and 9, respectively, shows the effect of increasing temperature on the percentage reduction in area and hydrogen atom concentration on the surface of the exposed specimens.

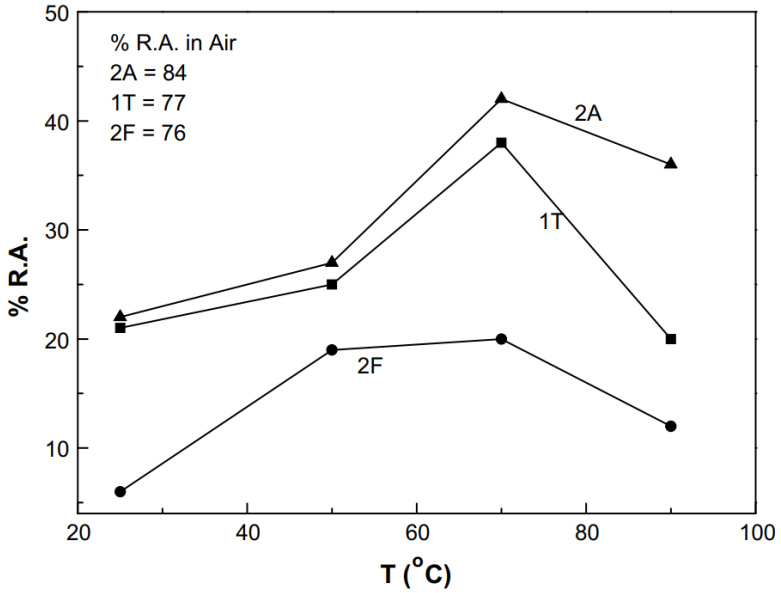

Figure 8. Effect of increasing temperature on percentage reduction in the area for the different microstructures: 2F (martensitic microstructure); 1T (ferritic/bainitic microstructure); 2A (ferritic microstructure) [61]. Reprinted with permission from [61], 2008, Elsevier.

It was observed that the steel with martensitic microstructure had the lowest SCC resistance at all temperatures, whereas the steels with ferritic and ferritic/bainitic microstructures showed less resistance at 25 °C. As shown in Figure 8, the SCC susceptibility decreased with increasing temperature for all microstructures from 25 to 70 °C; it then increased with further increases in temperature up to 90 °C.

As shown in Figure 9, the concentration of hydrogen atoms (C_0) increased with increasing temperature regardless of microstructure, but the increase is much higher for the ferritic/bainitic microstructure (1T). The highest concentrations of hydrogen atoms were observed on the 1T steels (ferritic/bainitic microstructure) and lowest C_0 values were observed for martensitic microstructure (2F). In summary, the martensitic steel showed a brittle type of fracture with trans-granular cracks. This shows a typical hydrogen embrittle-

ment type of failure, and in most cases, with clear evidence of anodic dissolution taking place on the surface of the specimens.

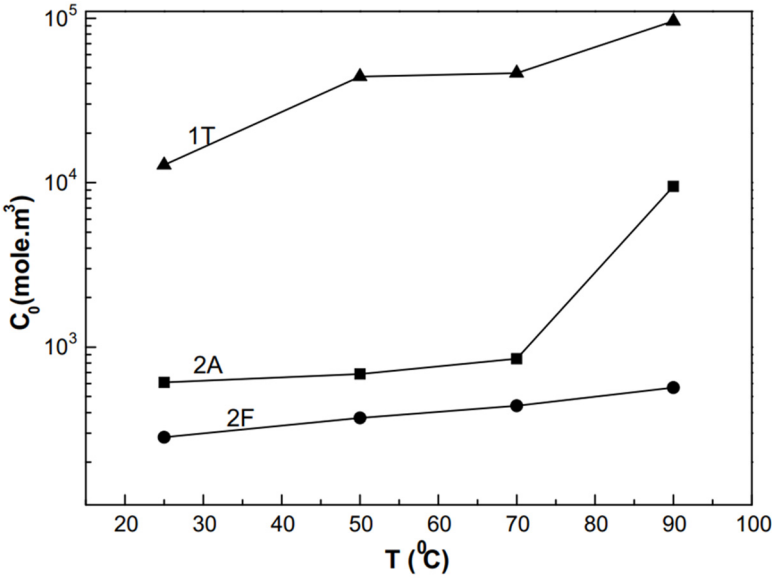

Figure 9. Effect of increasing temperature on hydrogen atom concentration (C_0) on the surface of the different steel microstructures: 2F (martensitic microstructure); 2A (ferritic microstructure); 1T (ferritic/bainitic microstructure) [61]. Reprinted with permission from [61], 2008, Elsevier.

According to the reviewed research articles on the SCC susceptibility of pipeline carbons steels exposed at different temperatures, it can be summarised that SCC susceptibility of the steels at a particular temperature depends on the type and composition of the corrosive medium and microstructure of the steel.

8. Effect of Applied Stress and Stress Application Techniques on SCC of Pipeline Steels

According to Fontana [6], the minimum stress required for cracking to occur on a metal or alloy depends on temperature, alloy composition and composition of corrosive environment. In some cases, cracking has been observed to occur with as low as 10% of the alloy's yield strength [6,11], while in other cases, cracking does not take place below about 70% of the material's yield strength [6]. The threshold stress for crack initiation was found to depend on the amount of carbon in the steel. Regular steels tend to be more susceptible to SCC, as their carbon content is lower than 0.1%, while ferritic steels that have chromium content of about 18 to 20 percent are highly resistant to SCC [9,11].

Gui et al. [62] conducted three tests in three different laboratories (round robin testing) to investigate the effect of aerated fuel grade ethanol at open circuit potential on susceptibility of notched X-46 carbon steel to SCC. The strain rates of 3.7×10^{-7} in/s, 4×10^{-7} in/s and 5×10^{-7} in/s were applied in the three laboratories. The tests results in the first two laboratories indicated that the exposed specimens are susceptible to SCC and observed a trans-granular mode of fracture. However, in the third laboratory, SCC was not observed on the specimen unless chloride was added into the ethanol solution. Lou et al. [63] reported that the presence of chloride ions and acetic acid in fuel grade ethanol facilitates SCC occurrence of carbon steels. Samusawa et al. [64] also observed that chloride concentration accelerates ethanol cracking under cyclic loading conditions. The observed phenomenon here is that the level of applied stress on a metal or alloy plays a vital role in its susceptibility to SCC and the concentration of chloride ions facilitates the occurrence of SCC on carbon steels.

Omura et al. [17] studied SCC susceptibility of API 5L X80 grade material in comparison with API 5L X65 by use of different stress application methods including SSRT test,

constant load test and cyclic loading test with applications of 85% and 100% of the materials Y.S. in cyclic loading test, 90% of the materials Y.S. in constant load test and 1×10^{-6} in/s in SSRT. The tests were conducted in NS4 solution with continued bubbling of 10% CO_2 and 90% N_2 with application of different cathodic potentials at a temperature of 25 °C. The tests results indicated that SCC occurred under the maximum applied stress of 100% Y.S. at −1000 mV (SCE) in the cyclic loading test, with no occurrence of SCC under 85% Y.S. at −1100 mV (SCE). No significant SCC occurrence was observed in the constant load tests under the applied stress of 90% Y.S. at a potential of −1250 mV (SCE). Similar results were reported by Samusawa et al. [64] when they investigated the environmental-assisted cracking resistance of API 5L X52 carbon steel in several simulated fuel grade ethanol (SFGE) under low frequency cyclic load and constant load applications. Maximum applied stresses of 105% and 110% of actual material yield strength were applied during the cyclic load tests and 110% Y.S. was applied during the constant load test. All tests were performed at a temperature of 23 ± 2 °C. The tests results revealed that in the simulated fuel grade ethanol, X52 carbon steel specimens fractured under the low-frequency cyclic loading conditions, but no fracture was observed under the constant load condition. A mixture of intergranular and trans-granular cracking mechanisms was observed on the fractured specimens under the cyclic load conditions. Lu and Luo [65] also observed similar results on X70 pipeline steel tested in NS4 solution under low-frequency cyclic load. The tests results show that an increase in applied stress level accelerates crack initiation on the specimens. However, crack propagation rates were found to be independent of the applied stress level. Furthermore, Contreras et al. [50] also revealed that the SCC susceptibility of X52 carbon steel tested in NS4 solution was found to increase with increasing yield stress and ultimate tensile stress (UTS).

Wang et al. [66] investigated the effect of pre-cyclic loading prior to corrosion exposure on API 5L X65 and X80 carbon steels in a near-neutral pH soil solution at open circuit potential of −740 mV (SCE) and at −50 mV (SCE) below E_{corr} (−790 mV (SCE)). A maximum stress of 80% Y.S. and 90% Y.S. was applied on the specimens during the pre-cyclic loading and constant load tests. This percentages of applied yield stress are chosen in order to simulate the actual loading condition in the field. The tests results revealed that pre-cyclic loading caused the formation of microcracks on the sample's surfaces during subsequent corrosion exposure under constant load and under mild cathodic polarization. No microcracks were observed on the specimens' surfaces at the open-circuit potential regardless of whether the samples were under constant load or cyclic load during the corrosion exposure because of uniform corrosion. For all specimens of both steels without pre-cyclic loading, no surface defects (micro cracks or pits) were observed after corrosion exposure under constant load (80% Y.S.) for 10 or 24 days at a potential of −790 mV (SCE). However, for all the specimens with pre-cyclic loading, microcracks were observed on the specimens' surfaces when exposed to the environment under cathodic polarization potential of −790 mV (SCE) at a constant load of 80% Y.S. and 90% Y.S.

In general, it can be summarised that the level of applied stress, stress concentration and fluctuating stress plays a vital role in SCC initiation and propagation of pipeline carbon steels. The presence of either or all of these factors accelerates the occurrence of SCC in pipeline carbons steels, especially in the presence of more aggressive corrosive environment such as, CO_2, H_2S, etc.

9. Effect of pH on Cracking Susceptibility of Pipeline Steels

The pH of a corrosive environment has profound influence on the rate at which corrosion occurs on metals or alloys and may also defend on the type of the metal [11]. An acidic medium with pH less than 5 tends to be aggressive and accelerates corrosion, while alkaline solutions are less corrosive and can easily form protective layers [21]. For example, the corrosion rate of metals such as zinc and iron is accelerated in low pH (acidic) medium [11]. Several studies have been carried out and reported on the influence of pH on

SCC susceptibility of pipeline carbon steels in various corrosive environments as discussed in subsequent paragraphs.

Contreras et al. [67] studied the susceptibility of API 5L X52 carbon steel to SCC by use of SSR technique at a strain rate of 1×10^{-6} in/s. The specimens were exposed in air and in NS4 solution with pH levels of 5, 8 and 10. The tests results indicated higher time to failure for specimens exposed in air, and lower time to failure was observed for specimens exposed in solution with pH 8. Figure 10 presents the variation of time to failure of the specimens in the different pH NS4 solutions. SEM results indicated ductile fracture on specimens exposed in air and in solution with pH 8 and 10, while brittle fracture with trans-granular appearance was observed on the specimens tested in the pH 5 solution. According to the calculated area reduction ratio (RRA) and time to failure ratio (TFR) specimens exposed to the NS4 solution with pH 5 are more susceptible to SCC. Figures 11 and 12, respectively, presents the SEM images of the brittle and ductile fracture observed on the exposed samples at pH 5 solution and in air.

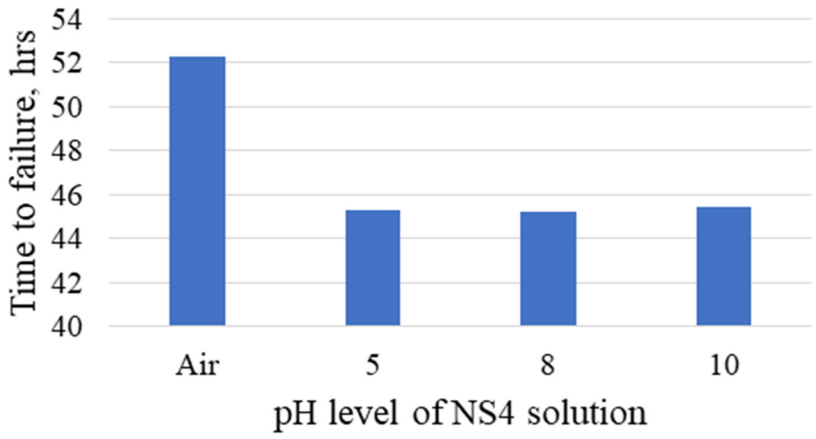

Figure 10. Variations in time to failure of the exposed X52 carbon steel in air and the different NS4 solution pH level. Data from [67].

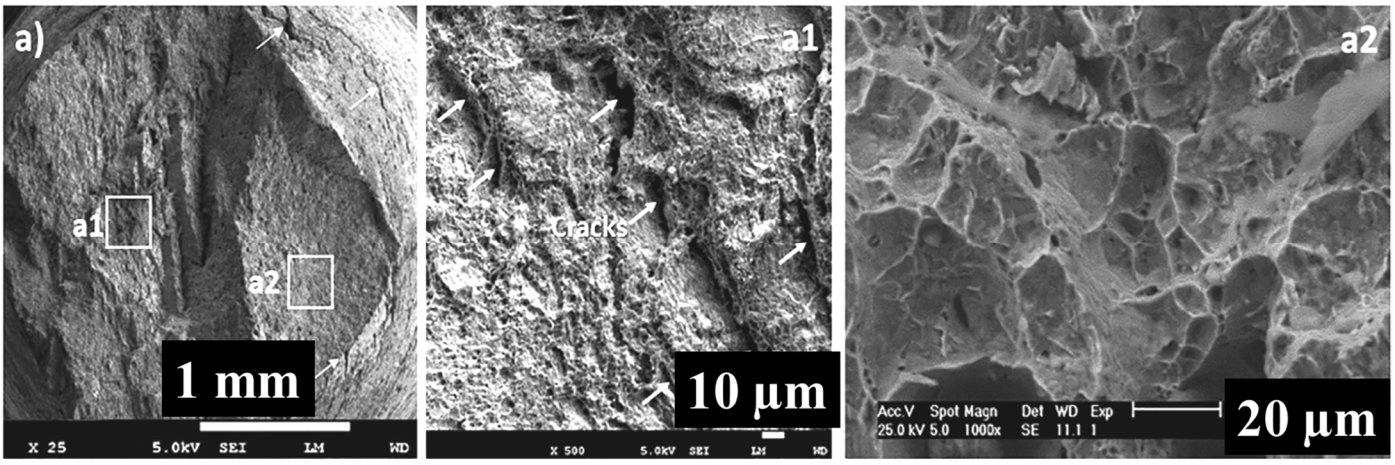

Figure 11. SEM images showing a brittle type of fracture with trans-granular appearance on the X52 exposed specimens in the NS4 solution at pH 5 [67].

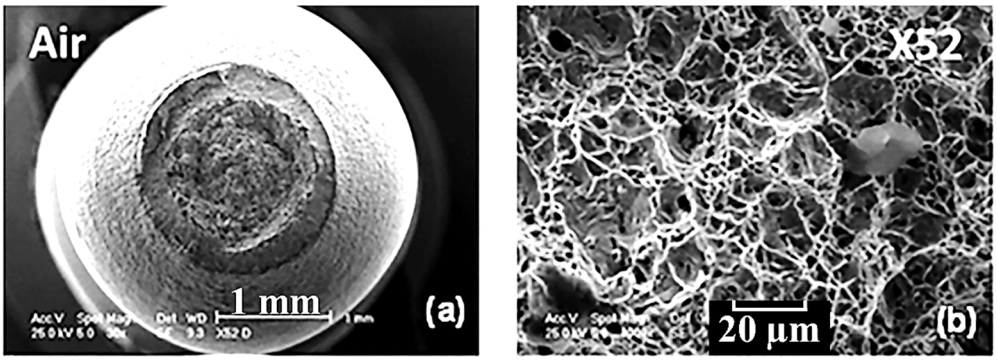

Figure 12. SEM images showing a ductile type of fracture on the X52 exposed specimens in air [67].

Figure 11a as presented above shows the specimens surface cracks with brittle fracture and faceted surface texture. Higher magnification image of the cracked section as shown in Figure 11a1 revealed that hydrogen atoms induce internal microcracks. Figure 11a2 shows a higher magnification image of the faceted section which revealed a typical trans- granular mode of fracture.

As shown in Figure 12a, the sample revealed a ductile fracture, which is characterized by a formation of neck prior to failure with extensive permanent plastic deformation. Figure 12b presents a higher magnification image of the fractured surface revealing ductile mode of fracture with trans-granular appearance.

Cui et al. [68] investigated the effect of pH value on electrochemical and SCC susceptibility of API 5L X70 carbon steel in NS4 solution by use of SSRT at a strain rate of 1×10^{-6} in/s. The specimens were exposed in air and NS4 solution with pH level of 4.0, 4.5, 5.0, 5.5, 6.0 and 6.8. Test solutions were continuously bubbled with 5% CO_2 and 95% N_2 throughout the duration of the tests. In general, the susceptibility of the samples to SCC changes with decreasing pH of the test solution. It was observed that when the pH value was decreased from 6.8 to 6, both cathodic reduction and anodic dissolution were increased. Acceleration of the cathodic reduction was observed with further decrease in the pH value of the solution. When the solution pH decreases from 6.8 to 5.5, SCC susceptibility decreases because of the enhancement of the anodic dissolution. Conversely, when the solution pH decreases from 5.5 to 4.0, SCC susceptibility increases steadily because of the acceleration of the cathodic reactions. In conclusion, as the solution pH decreases, secondary cracks show no clear variations until the pH value reduces to 4.0. It was observed that the secondary cracks became wider and deeper in the solution with the pH value of 4.0, and hence, the SCC susceptibility of the specimen was higher. The tests results showed a clear change in the open circuit potential of the specimens in the various solution pH value. Figure 13 shows the variations in the OCP value with changing pH values. It was observed that the OCP moves positively as the solution pH decreases. Similar results of change in OCP values with decreasing pH level in acidic soil solutions were observed by Liu et al. [69] while conducting SCC susceptibility of X70 pipeline steel. Figure 14 shows the variations in OCP values with decreasing pH values of the acidic solutions. Alfantazi et al. [70,71] also reported the electrochemical behaviour of X100 pipeline steel in NS4 solution and in chloride-containing CO_2-saturated solution of pH levels between 4.7 and 9. The results also showed that the open circuit potential values decreased with increasing pH level, hence contributing to the decrease in the cathodic reduction reactions at higher pH values [70]. The corrosion rate was observed to increase with decreasing pH values [71].

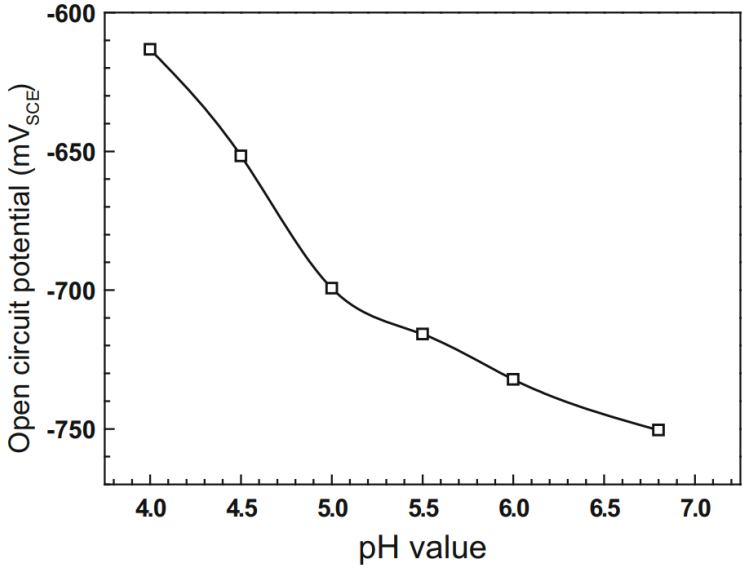

Figure 13. Variations of open circuit potential of the X70 samples in the different pH NS4 solutions [68]. Reprinted with permission from [68], 2015, Springer nature.

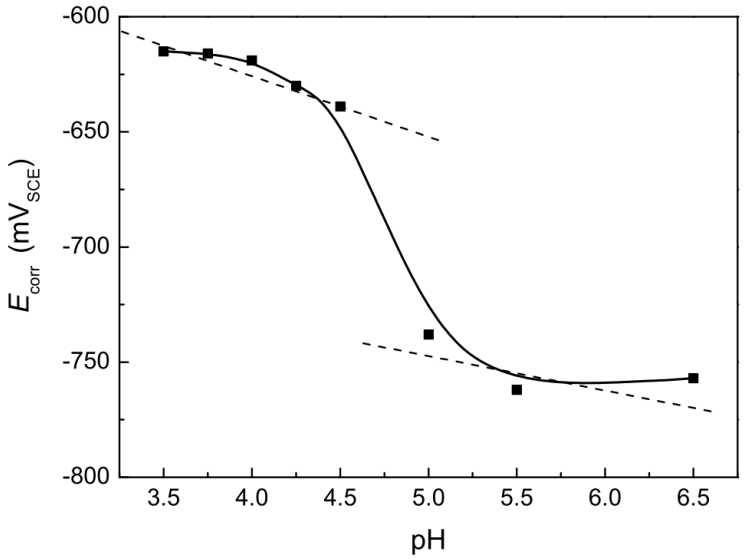

Figure 14. Variations of open circuit potential of the X70 samples in the different pH acidic soil solutions [69]. Reprinted with permission from [69], 2013, Springer nature.

Nesic et al. [28] assessed the electrochemical behaviour of mild steel in aqueous CO_2 medium of pH range 4–6. The tests results showed that pH level had no clear effect on anodic dissolution of the specimens in the CO_2 solutions. Chen et al. [72] evaluated the susceptibility of API 5L X70 carbon steel to SCC in four different soil samples excavated from underground where pipelines are buried. Different concentrations of CO_2/N_2 gas mixtures were introduced during the tests. The tests results showed that the SCC susceptibility of the samples increased gradually as the soil pH increased from 5.5 to 7.0. Liu et al. [69] studied the effect of pH value in the range from 3.5 to 6.5 on SCC susceptibility of API 5L X70 pipeline steel in simulated acidic synthetic soil media. The carbon steel was observed to show the highest SCC susceptibility under pH value of 4.5; this is because of the strongest synergistic effect of hydrogen embrittlement and anodic dissolution. It was observed that when the solution pH was greater or lower than 4.5, SCC susceptibility decreased [69].

Parkins et al. [73] assessed the susceptibility of different pipeline steels (X52, X60 and X65) to SCC in NS4 solution with various pH values of 8.3, 6.3 and 5.1. Hydrogen perme-

ation tests were carried out on the three different pipeline steel samples at open circuit potential and at potentials of −700 mV (SCE) and −800 mV (SCE) below the corrosion potential. All tests were conducted at temperatures of 23 ± 1 °C. The tests results showed that irrespective of the steel grade, hydrogen concentration on the sample surfaces increases with decreasing pH value in near-neutral environments within the vicinity of open circuit potential and the applied potentials. However, hydrogen embrittlement is not exclusively involved in the SCC occurrence since there is clear evidence of anodic dissolution associated with the cracking of the pipeline steels. Jeffrey et al. [53] also reported that lower pH value led to higher absorbed hydrogen concentrations on X-65 sample surfaces exposed in a near-neutral carbonate/bicarbonate solutions with increasing CO_2 concentrations. Figure 15a,b, respectively, presents the variations in hydrogen concentration values on the specimens surfaces at −700 mV (SCE) and −800 mV (SCE) with varying pH of the NS4 solutions.

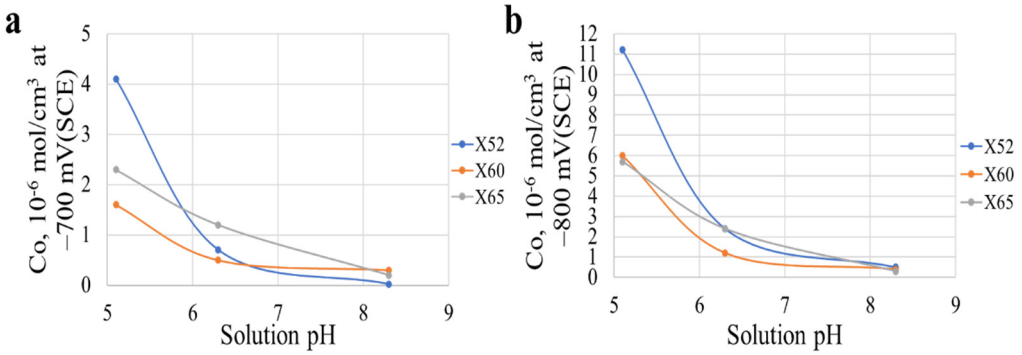

Figure 15. Variations in hydrogen concentration values on the exposed carbon steels at varying pH of the NS4 solution: (**a**) at applied potential of −700 mV (SCE); (**b**) at applied potential of −800 mV (SCE). Data from [73].

In summary, it was observed that despite all the current research, the effect of solution pH on SCC behaviour of pipeline steels is still not clear. However, it can be stated that most carbon steels are more susceptible to SCC under pH value of 5 regardless of the type of solution. Generally, it was observed that a higher CO_2 concentration in a solution leads to a lower pH value. This in turn increases the concentration of hydrogen on the metal surfaces, thus enhancing its susceptibility to SCC.

10. Conclusions

Based on the above reviewed research articles investigating the factors affecting SCC susceptibility of pipeline carbon steels, the following conclusions can be made:

(1) Pipeline carbon steels with water quenched, quenched and tempered heat treatment and consist of acicular ferrite, bainitic ferrite or martensitic microstructure are more susceptible to SCC irrespective of corrosive environment and composition.
(2) The level of applied stress, stress concentration and fluctuating stress plays a vital role in SCC initiation and propagation for pipeline carbon steels.
(3) It can be concluded that SCC susceptibility of the carbon steels at a particular temperature depends on the type and composition of the corrosive medium and microstructure of the steel.
(4) It was observed that SCC of pipeline steels in a near-neutral pH condition varies with solution composition, concentration of oxidizers and their applied partial pressure. It is clear that with increasing CO_2 concentration, polarization resistance (R_p) decreases, which in turn increases corrosion rate, hence facilitating SCC occurrence. The severity of SCC occurrence increases with increasing applied cathodic potential.
(5) According to the reviewed articles, the effect of solution pH on SCC behaviour of pipeline steels is not clear. However, most carbon steels are more susceptible to SCC between pH values of 4–5 regardless of the type of environment. It was observed

that open circuit potential values decreased with increasing pH level. Generally, it was observed that higher CO_2 concentration in a solution leads to lower pH value. This in turn increases the concentration of hydrogen on the metal/alloy surfaces, thus enhancing susceptibility to SCC.

(6) In general, the mechanism for crack initiation and propagation in a near-neutral solution with varying concentrations of O_2 and CO_2 constitutes anodic dissolution and hydrogen embrittlement.

11. Research Suggestions

Based on the above reviewed articles, the following suggestions are observed for future research considerations:

(1) Systematic studies should be carried out to clearly understand the effect of temperature on SCC of pipeline steels with regard to different microstructures in a near-neutral pH condition.

(2) The changes in the electrochemical reactions and the SCC susceptibility of pipeline carbon steels over different solution pH values should be further researched.

Author Contributions: Conceptualization, S.A.A., S.M. and J.S.; methodology, S.A.A., S.M. and J.S.; investigation, S.A.A.; data curation, S.A.A.; writing—original draft preparation, S.A.A.; writing—review and editing, J.S. and S.M.; supervision, J.S. and S.M.; project administration, J.S.; funding acquisition, S.A.A. All authors have read and agreed to the published version of the manuscript.

Funding: This research and APC was funded by Cranfield University.

Institutional Review Board Statement: Not applicable.

Informed Consent Statement: Not applicable.

Data Availability Statement: Scopus, OnePetro, Knovel, ScienceDirect.

Conflicts of Interest: The authors declare no conflict of interest.

References

1. Liu, H. Introduction. In *Pipeline Engineering*; Lewis Publishers: Boca Raton, FL, USA; CRC Press Company LLC.: Washington, DC, USA, 2003; pp. 1–3.
2. Menon, E.S. Corrosion Protection. In *Pipeline Planning and Construction Field Manual*; Gulf Professional Publishers: Houston, TX, USA; Elsevier: Amsterdam, The Netherlands, 2011; pp. 293–297.
3. Aloqaily, A. Foreword and Book Description. In *Cross Country Pipeline Risk Assessments and Mitigation Strategies*; Gulf Professional Publishing: Houston, TX, USA, 2018; p. 334.
4. Orazem, M.E. Understanding and Managing Corrosion Processes. In *Underground Pipeline Corrosion: Detection, Analysis and Prevention*; Woodhead Publishing Ltd.: Sawston, UK, 2014; pp. 1–32.
5. Singh, R. Corrosion and Corrosion Protection. In *Pipeline Integrity: Management and Risk Evaluation*; Gulf Professional Publishing: Houston, TX, USA; Elsevier: Amsterdam, The Netherlands, 2017; pp. 243–253.
6. Fontana, M.G. Stress Corrosion. In *Corrosion Engineering*, 3rd ed.; McGraw-Hill International Book Company: Columbus, OH, USA, 1987; pp. 109–138.
7. Palmer, A.C.; King, R.A. Risks, Accidents and Repairs. In *Subsea Pipeline Engineering*; PennWell Publishing Company: Tulsa, OK, USA, 2008; pp. 507–522.
8. Villanueva-balsera, J.; Rodriguez-perez, F. Methods to Evaluate Corrosion in Buried Steel Structures: A Review. *Metals* **2018**, *8*, 334.
9. Cicek, V. Types of Corrosion. Non-uniform Corr. In *Corrosion Engineering*; John Wiley and Sons: Hoboken, NJ, USA, 2014; pp. 67–70.
10. Davis, J.R. Forms of Corrosion: Recognition and Prevention. In *Corrosion-Understanding the Basics*; ASM International: Almere, TheNetherlands, 2000; pp. 100–155.
11. Sastri, V.S. Introduction and forms of Corrosion. In *Challenges in Corrosion: Costs, Causes, Consequences, and Control*; John Wiley & Sons Inc.: Hoboken, NJ, USA, 2015; pp. 1–95.
12. Papavinasam, S. Monitoring Internal Corrosion. In *Corrosion Control in the Oil and Gas Industry*; Gulf Professional Publishing: Houston, TX, USA; Elsevier: Amsterdam, The Netherlands, 2014; pp. 425–514.

13. Bueno, A.H.S.; Castro, B.B.; Ponciano, J.A.C. Laboratory Evaluation of Soil Stress Corrosion Cracking and Hydrogen Embrittlement of API Grade Steels. In Proceedings of the International Pipeline Conference, Calgary, AB, Canada, 4–8 October 2004; pp. 1–6.
14. Torres-Islas, A.; Gonzalez-Rodriguez, J.G.; Uruchurtu, J.; Serna, S. Stress Corrosion Cracking Study of Microalloyed Pipeline Steels in Dilute $NaHCO_3$ Solutions. *Corros. Sci.* **2008**, *50*, 2831–2839. [CrossRef]
15. Bueno, A.H.S.; Moreira, E.D.; Gomes, J.A.C.P. Evaluation of Stress Corrosion Cracking and Hydrogen Embrittlement in an API Grade Steel. *Eng. Fail. Anal.* **2014**, *36*, 423–431. [CrossRef]
16. Majchrowicz, K.; Brynk, T.; Wieczorek, M.; Miedzi, D. Exploring the Susceptibility of P110 Pipeline Steel to Stress Cor-rosion Cracking in CO_2-Rich Environments. *Eng. Fail. Anal.* **2019**, *104*, 471–479. [CrossRef]
17. Omura, T.; Amaya, H.; Asahi, H.; Sawamura, M.; Kimura, M.; Ishikawa, N. Near Neutral SCC Properties of Grade X80 Linepipe. In Proceedings of the NACE-International Corrosion Conference and Expo, Atlanta, GA, USA, 22–26 March 2009; Volume 09092, pp. 1–16.
18. Revie, R.W. Stress Cracking. Basics of Corrosion Science and Engineering. In *Uhlig's Corrosion Handbook*, 3rd ed.; John Wiley and Sons: Hoboken, NJ, USA, 2011; pp. 171–183.
19. Popoola, L.T.; Grema, A.S.; Latinwo, G.K.; Gutti, B.; Balogun, A.S. Corrosion Problems During Oil and Gas Production and its Mitigation. *Int. J. Ind. Chem.* **2013**, *4*, 35–40. [CrossRef]
20. Kreysa, G.; Schütze, M. *Dechema Corrosion Handbook-Revised and Extended*, 2nd ed.; Dechema: Frankfurt am Main, Germany, 2008.
21. Davies, P.J.B.; Scott, M. Environmental Assited Cracking. In *Guide to the Use of Materials in Waters*; NACE International: Houston, TX, USA, 2003; pp. 50–53.
22. Johnson, J.T.; Durr, C.L.; Beavers, J.A.; Delanty, B.S.; Pipelines, T. Effects of O_2 and CO_2 on Near-Neutral-pH Stress Corrosion Crack Propagation. In Proceedings of the NACE—International Corrosion Conference Series, Orlando, FL, USA, 26–31 March 2000; Volume 2000-March, No. 356. pp. 1–22.
23. Bodlos, R. Detailed microstructure characterization of a grade X70 steel modified with TiO_2 using friction stir processing. Master's Thesis, Graz University of Technology, Graz, Austria, 2018; pp. 4–10.
24. Bulger, J.; Luo, J. Effect of Microstructure on Near-Neutral-pH SCC. In Proceedings of the 2000 International Pipeline Conference, Calgary, AB, Canada, 1–5 October 2000; Volume 2, pp. 947–952.
25. Koch, G.; Varney, J.; Thompson, N.; Moghissi, O.; Gould, M.; Payer, J. *International Measures of Prevention, Application and Economics of Corrosion Technologies Study*; NACE International: Houston, TX, USA, 2016.
26. Cole, I.S.; Corrigan, P.; Sim, S.; Birbilis, N. Corrosion of Pipelines used for CO_2 Transport n CCS: Is it a Real Problem? *Int. J. Greenh. Gas Control* **2011**, *5*, 749–756. [CrossRef]
27. Wei, L.; Pang, X.; Gao, K. Effect of Small Amount of H2S on the Corrosion Behavior of Carbon Steel in the Dynamic Supercritical CO2 Environments. *Corros. Sci.* **2016**, *103*, 132–144. [CrossRef]
28. Nesic, S.; Postlethwaite, J.; Olsen, S. An Electrochemical Model for Prediction of Corrosion of Mild Steel in Aqueous Carbon Dioxide Solution. *Corros. Sci.* **1996**, *52*, 280–294. [CrossRef]
29. Mu, L.J.; Zhao, W.Z. Investigation on Carbon Dioxide Corrosion Behaviour of HP13Cr110 Stainless Steel in Simulated Stratum Water. *Corros. Sci.* **2010**, *52*, 82–89. [CrossRef]
30. Bhattacharyya, B. Recent Advancements in EMM for Micro and Nanofabrication. In *Electrochemical Micromachining for Nanofabrication, MEMS and Nanotechnology*; William Andrew Publishers, ScienceDirect: Norwich, NY, USA, 2015; pp. 219–240.
31. Bai, Y.; Bai, Q. Use of High Strength Steel. In *Subsea Pipelines and Risers*; Elsevier Ltd.: Oxford, UK, 2005; pp. 565–571.
32. Bai, Y.; Bai, Q. Usage of High-Strength Steel Line Pipes. In *Subsea Pipeline Design, Analysis, and Installation*; Gulf Professional Publishing: London, UK, 2014; pp. 676–682.
33. Silva, S.C.; Souza, E.A.; Pessu, F.; Hua, Y.; Barker, R.; Neville, A.; Gomes, J.A.D.C.P. Cracking Mechanism in API 5L X65 Steel in a CO_2-Saturated Environment. *Eng. Fail. Anal.* **2019**, *99*, 273–291. [CrossRef]
34. Contreras, A.; Espinosa-Medina, M.A.; Salazar, M. Assessement of SCC Susceptibility of Supermatensitic Stainless Steel Through Slow Strain Rate Tests. In Proceedings of the 7th International Pipeline Conference, Calgary, AB, Canada, 29 September–3 October 2008; pp. 547–555.
35. Hoeppner, D.W. Structural Integrity Considerations in Engineering Design, Fatigue and Damage. In *Tolerance Considerations in Design*; John Wiley & Sons: Hoboken, NJ, USA, 2011; Volume 1, pp. 50–105.
36. Baboian, R. Corrosion Testing. In *NACE Corrosion Engineer's Reference Book*, 4th ed.; NACE International: Houston, TX, USA, 2016; pp. 115–160.
37. Hwang, B.; Kim, Y.M.; Lee, S.; Kim, N.J.; Ahn, S.S. Correlation of Microstructure and Fracture Properties of API X70 Pipe-line Steels. Research gate. *Metall. Mater. Trans. A* **2005**, *36*, 725–739. [CrossRef]
38. Natividad, C.; Falcon, L. Mechanical and Metallurgical Properties of Grade X70 Steel Linepipe Produced by Non-conventional Heat Treatment. In *Characterization of Metals and Alloys*; Springer: Berlin/Heidelberg, Germany, 2017; pp. 3–11.
39. Thomson, J.K.; Pawel, S.J. A Comparison of the C-Ring Test and the Jones Test as Standard Practice Test Methods for Studying Stress Corrosion Cracking in Ferritic Steels. In Proceedings of the NACE-International Corrosion Conference and Expo, Dallas, TX, USA, 15–19 March 2015; Paper No. 5670. pp. 1–11.
40. Park, I.; Lee, C.; Hwang, S.; Kim, H.; Kim, J.; Box, P.O. Caustic Stress Corrosion Cracking of Alloys 600 and 690 with NaOH Concentrations. *Met. Mater. Int.* **2005**, *11*, 401–409. [CrossRef]

41. Gonzalez-Rodriguez, J.G.; Casales, M.; Salinas-Bravo, V.M.; Albarran, J.L.; Martinez, L. Effect of Microstructure on the Stress Corrosion Cracking of X-80 Pipeline Steel in Diluted Sodium Bicarbonate Solutions. *Corros. Sci.* **2002**, *58*, 584–590. [CrossRef]
42. Liu, Z.Y.; Li, X.G.; Du, C.W.; Zhai, G.L.; Cheng, Y.F. Stress corrosion cracking behavior of X70 pipe steel in an acidic soil environment. *Corros. Sci.* **2008**, *50*, 2251–2257. [CrossRef]
43. Zhang, L.; Li, X.; Du, C.; Huang, Y. Effects of Temperature and Applied Potential on Stress Corrosion of X70 Pipeline Steel in Simulated Soil Solution. *Jinshu Rechuli/Heat Treat. Met.* **2015**, *40*, 183–187.
44. Luo, J.L.; Bulger, J.T.; Lu, B.T. Microstructural Effect on Near-Neutral pH Stress Corrosion Cracking Resistance of Pipe-line Steels. *J. Mater. Sci.* **2006**, *5*, 5001–5005.
45. Zhu, M.; Liu, Z.; Du, C.; Li, X.; Li, J.; Li, Q.; JIA, J. Stress Corrosion Cracking Behavior and Mechanism of X65 and X80 Pipeline Steels in High pH Solution. *Jinshu Xuebao/Acta Metall. Sin.* **2013**, *49*, 1590–1596. [CrossRef]
46. Lu, B.T.; Luo, J.L. Relationship Between Yield Strength and Near-Neutral pH Stress Corrosion Cracking Resistance of Pipeline Steels—An Effect of Microstructure. *Corros. Sci.* **2006**, *62*, 129–140. [CrossRef]
47. Hafeez, M.A.; Inam, A.; Farooq, A. Mechanical and corrosion properties of medium carbon low alloy steel after cyclic quenching and tempering heat–treatments. *Mater. Res. Express* **2020**, *7*, 1–12. [CrossRef]
48. Kang, J.; Zhang, F.C.; Yang, X.W.; Lv, B.; Wu, K.M. Effect of tempering on the microstructure and mechanical properties of a medium carbon bainitic steel. *Mater. Sci. Eng. A* **2017**, *686*, 150–159. [CrossRef]
49. Rebak, R.B.; Xia, Z.; Safruddin, R. Effect of Solution Composition and Electrochemical Potential on Stress Corrosion Cracking of X-52 Pipeline Steel. *Corros. Sci.* **1996**, *52*, 396–405. [CrossRef]
50. Contreras, A.; Hernández, S.L.; Orozcocruz, R.; Galvan-martínez, R. Mechanical and Environmental Effects on Stress Corrosion Cracking of Low Carbon Pipeline Steel in a Soil Solution. *Mater. Des.* **2012**, *35*, 281–289. [CrossRef]
51. Zhang, L.; Shen, H.; Xing, Y.; Cao, W.; Fang, Y.; Lu, M. Investigation of Hydrogen Embrittlement of High Strength Pipe-line Steels under Cathodic Protection. In Proceedings of the NACE-International Corrosion Conference and Expo, Houston, TX, USA, 26–30 March 2017; Volume 9255, pp. 1–14.
52. Zhang, L.; Li, X.G.; Du, C.W.; Cheng, Y.F. Corrosion and Stress Corrosion Cracking Behavior of X70 Pipeline Steel in a CO_2-Containing Solution. *ASM Int.* **2009**, *18*, 319–323. [CrossRef]
53. Xie, J.; Foy, C.; Worthingham, R.; Piazza, M. Environmental Effects on the Susceptibility and Crack Growth of Near Neutral pH Stress Corrosion cracking. In Proceedings of the NACE-International Corrosion Conference and Expo, San Antonio, TX, USA, 14–18 March 2010; Volume 10297, pp. 1–11.
54. Asher, S.L.; Singh, P.M. Investigating the Impact of Environment on Transgranular Stress Corrosion Cracking of Pipeline Steels. In Proceedings of the NACE-International Corrosion Conference and Expo, Houston, TX, USA, 26–30 March 2017; Volume 7130, pp. 1–13.
55. Gu, B.; Yu, W.Z.; Luo, J.L.; Mao, X. Transgranular Stress Corrosion Cracking of X-80 and X-52 Pipeline Steels in Dilute Aqueous Solution with Near-Neutral pH. *Corros. J.* **1999**, *55*, 312–318. [CrossRef]
56. Davies, M.; Scott, P.J.B. Corrosion of Metals. In *Oilfield Water Technology*; NACE Int.: Houston, TX, USA, 2006; pp. 73–100.
57. Contreras, A.; Hernández, S.L.; Galván-Martínez, R. Effect of pH and temperature on stress corrosion cracking of API X60 pipeline steel. In Proceedings of the Materials Research Society Symposium Proceedings, Cancun, Mexico, 15–19 August 2010; Volume 175, pp. 43–52.
58. Asher, S.; Singh, P.M.; Colwell, J.A.; Leis, B.N. Stress Corrosion Cracking of Pipeline Steel in Near-Neutral pH Environments. In Proceedings of the 61st Annual Corrosion Conference and Expo, NACE-International Corrosion Conference and Expo, Houston, TX, USA, 2006; Volume 6175, pp. 1–10.
59. Cundong, Y.E.; Dejun, K.; Lei, Z. Effects of temperature on stress corrosion of X70 pipeline steel in solution with oxygen. *J. Cent. South Univ. (Sci. Technol.)* **2015**, *46*, 2432–2438.
60. Fragiel, A.; Serna, S.; Malo-Tamayo, J.; Silva, P.; Campillo, B.; Martínez-Martínez, E.; Perez, R. Effect of Microstructure and Temperature on the Stress Corrosion Cracking of Two Microalloyed Pipeline Steels in H_2S Environment for Gas Transport. *Eng. Fail. Anal.* **2019**, *105*, 1055–1068. [CrossRef]
61. Ramírez, E.; González-Rodriguez, J.G.; Torres-Islas, A.; Serna, S.; Campillo, B.; Dominguez-Patiño, G. Effect of Micro-structure on the Sulphide Stress Cracking Susceptibility of a High Strength Pipeline Steel. *Corros. Sci.* **2008**, *50*, 3534–3541. [CrossRef]
62. Gui, F.; Trillo, E. Effect of Ethanol Chemistry on SCC of Carbon Steel: Results of a Round Robin Testing. In Proceedings of the IPC: 8th International Pipeline Conference, Calgary, AB, Canada, 27 September–1 October 2010; pp. 1–5.
63. Lou, X.; Yang, D.; Singh, P.M. Effect of Ethanol Chemistry on Stress Corrosion Cracking of Carbon Steel in Fuel-Grade Ethanol. *Corros. J.* **2009**, *65*, 785–797. [CrossRef]
64. Samusawa, I.; Shiotanib, K.; Kami, C. The Influence of Cyclic Load on Environmentally Assisted Cracking of Carbon Steel in Simulated Fuel Grade Ethanol. *Corros. Sci.* **2016**, *108*, 76–84. [CrossRef]
65. Lu, B.T.; Luo, J.L. Crack Initiation and Early Propagation of X70 Steel in Simulated Near-Neutral pH Groundwater. *Corro. NACE Int.* **2006**, *62*, 723–731. [CrossRef]
66. Wang, S.; Chen, W.; King, F.; Jack, T.R.; Fessler, R.R. Precyclic-Loading-Induced Stress Corrosion Cracking of Pipeline Steels in a Near-Neutral-pH Soil Environment. *Corros. J.* **2002**, *58*, 526–534. [CrossRef]
67. Contreras, A.; Salazar, M.; Carmona, A. Electrochemical Noise for Detection of Stress Corrosion Cracking of Low Carbon Steel Exposed to Synthetic Soil Solution. *Mater. Res.* **2017**, *20*, 1201–1210. [CrossRef]

68. Cui, Z.Y.; Liu, Z.Y.; Wang, L.W.; Ma, H.C.; Du, C.W.; Li, X.G.; Wang, X. Effect of pH Value on the Electrochemical and Stress Corrosion Cracking Behavior of X70 Pipeline Steel in the Dilute Bicarbonate Solutions. *ASM Int.* **2015**, *24*, 4400–4408. [CrossRef]
69. Liu, Z.; Du, C.; Zhang, X.; Wang, F.; Li, X. Effect of pH Value on Stress Corrosion Cracking of X70 Pipeline Steel in Acidic Soil Environment. *Acta Metall. Sin.* **2013**, *26*, 489–496. [CrossRef]
70. Gadala, I.M.; Alfantazi, A. Electrochemical behavior of API-X100 pipeline steel in NS4, near-neutral, and mildly alkaline pH simulated soil solutions. *Corros. Sci.* **2014**, *82*, 45–57. [CrossRef]
71. Eliyan, F.F.; Alfantazi, A. Electrochemical Investigations on the Corrosion Behavior and Corrosion Natural Inhibition of API-X100 Pipeline Steel in Acetic Acid and Chloride-Containing CO_2-Saturated Media. *J. Appl. Electrochem.* **2012**, *42*, 233–248. [CrossRef]
72. Chen, W.; King, F.; Jack, T.R.; Wilmott, M.J. Environmental Aspects of Near-Neutral pH Stress Corrosion Cracking of Pipeline Steel. *Met. Mater. Trans. A* **2002**, *33A*, 1429–1436. [CrossRef]
73. Parkins, R.N.; Beavers, J.A. Some Effects of Strain Rate on the Transgranular Stress Corrosion Cracking of Ferritic Steels in Dilute Near-Neutral-pH Solutions. *Corros. Sci.* **2003**, *59*, 258–273. [CrossRef]